Frontiers in Heat and Mass Transfer (FHMT), 18, 31 (2022)
DOI: 10.5098/hmt.18.31

Global Digital Central
ISSN: 2151-8629

Frontiers in Heat and Mass Transfer

Available at www.ThermalFluidsCentral.org

# CONVECTIVE HEAT TRANSFER IN A SQUARE CAVITY WITH EMBEDDED CIRCULAR HEATED BLOCK AT DIFFERENT POSITIONS

O. M. Oyewola [a,b,*] S. I. Afolabi [b], O. S. Ismail [b], M.O. Olasinde [b]

[a] *School of Mechanical Engineering, Fiji National University, Suva, Fiji*
[b] *Department of Mechanical Engineering, University of Ibadan, Ibadan, Nigeria*

## ABSTRACT

Finite element method is adopted in analyzing a two dimensional partial differential equations of Navier Stokes that governs mass, momentum and energy for a convective heat transfer problem within a square cavity. The cavity walls kept at constant cold temperature except for the right wall being adiabatic. With an embedded circular heated block located in the cavity, simulations are performed to determine the effect of the position of the block at the top, middle and bottom of the cavity on natural convection. The experiments are carried out for different values of Rayleigh number varying from $10^3$ – $10^6$ by using a COMSOL multiphysics software. The results are obtained in terms of streamline formation, temperature contours as well as Nusselt number. The results show that the position of the embedded hot circular body is strongly dependent on the fluid flow characteristics and thermal fields within the cavity. At a fixed Rayleigh number, the heat transfer coefficient dramatically increases when the circular heated block is embedded at the top position of the cavity and Nusselt number reaches the maximum around the hot circular block either at the top, middle or bottom position of the embedded body inside the cavity.

**Keywords**: Natural convection, Square cavity, Embedded circular block, Heat transfer, Rayleigh number.

## 1. INTRODUCTION

The mechanism of heat transfer by natural convection in modern day technology is essential due to its significant applications in engineering (Boonloi and Jedsadaratanachai, (2022); Kumari *et al.,* (2021); Saddam (2020)). Several numerical experiments have been carried out in cavities containing embedded block in various geometries and configurations especially in building system such as walls, windows or in electronic components cavities, these embedded solid block may serve as obstacle to reduce the flow by reducing the rate of heat transfer across the cavity (Oyewola, *et al.,* (2021); Ali and Jalal (2020); Ghobena and Hussein (2022)). Contrary, with a relatively high thermal conductivity of the solid block, heat transfer may be enhanced.

Several studies in the literature have been reviewed on natural convection in square cavities with various geometrical conditions and boundary parameters (House *et al.,* (1990); Oyewola, *et al.,* (2021); Ali and Jalal (2020); Ghobena and Hussein (2022); Flilihi *et al.,* (2021)). For example, House *et al.* (1990) analyzed the impact of natural convection in an enclosure with square heated body at the middle, with considerations on convectional parameters. They discovered that the heat transfer rate in the cavity was increased or reduced depending whether thermal conductivity ratio is greater or lesser than unity. Similarly, Ha *et al.* (2002) investigated a two-dimensional solution for unsteady state natural convection in a cavity containing a square body at the center, results revealed that at low Rayleigh number, temperature field and fluid flow maintained steady and symmetrical pattern but as it progresses to high Rayleigh number, the situation became unsteady and nonsymmetrical. Moreover, Shih *et al.* (2009) reported the numerical analysis of periodic state of laminar flow and rate of heat transfer in a square cavity due to rectangular rotating object. The authors found that with a bigger triangle adiabatic object, the performance of rate of heat transfer is enhanced. Further, Mousa (2010) conducted an experiment to model the laminar buoyancy effect of natural convection in a square cavity with a block inserted. The author discovered that heat transfer rate reduces with increasing aspect ratio of adiabatic square block for low Rayleigh numbers, while it increases as the adiabatic square block aspect ratio increases. In their numerical studies, Kandaswamy *et al.* (2007) observed the natural convection in a square cavity containing hot plate. It was gathered that rate of heat transfer increases vertically and horizontally for all increasing value of Grashof number, whereas the heat transfer increases with increase aspect ratio of the hot thin plate present. Chowdhury *et al.* (2005) numerically analyzed heat transfer in triangular cavities containing fluid saturated porous medium with a circular body in the presence of heat generation. Their results indicated that fluid flow and temperature field dramatically influenced the presence of circular body and heat transfer coefficient worsened as the size of the circular body and heat generation increases. It worth nothing that Merrikh and Mohamad (2001) investigated the effect of six square shaped solid objects on the natural convection in a rectangular enclosure of aspect ratio 2. They discovered that heat transfer rate was reduced as a result of blockage effects when the solid bodies are closed to the walls of the differentially heated cavity. In another perspective, Roslan *et al.* (2014) examined conjugate natural convection heat transfer in a differentially heated square cavity having a conductive polygon object. Their results showed an increase in size of the solid polygon. However, exceeding the critical value, heat transfer rate tends to reduce. Parvin and Nasrin (2011) studied heat transfer and fluid flow behavior for MHD natural convection in a cavity with hot obstacle. They observed that flow pattern and temperature field strongly depend on the Rayleigh number as well as Hartmann number, Nusselt number and diameter of circular body. In addition, Kakali *et al.* (2019) investigated the effect of different sizes and configurations of diamond shaped heated block on natural convection in a square cavity. The conclusions that stem out of their work indicated

* Corresponding author. Email: olanrewaju.oyewola@fnu.ac.fj

Global Digital Central
ISSN: 2151-8629

that average temperature increases as the size of the heated block increases, the average Nusselt reduces and also the region dominated by natural convection increases as the size of the block increases.

From the foregoing extensive literature review, it appears no substantial effort has been made on determining the effect of position of embedded circular heated block within a square cavity. In that respect, the present work focuses on the convective heat transfer in a square cavity with embedded circular heated block at various positions in the cavity. This is of practical interest. For example, major application of this phenomenon is employed in horizontal and vertical configuration of radiator because of its importance in regulating the temperature of air in heating and integrated cooling system of cavities. This paper will further improve our understanding on the study of heat transfer in fluid thermal management and design of engineering system.

## 2. NUMERICAL EQUATIONS AND PROBLEM ANALYSIS

Fig. 1 represents the schematic of a square cavity with embedded circular heated block, the fluid flow and heat transfer are assumed to be two-dimensional while the vertical walls are kept at constant cold temperature except the right wall which is insulated. The circular block is maintained at a uniform hot temperature. Free space area within the cavity are filled with incompressible Newtonian fluid which experience expansion and contraction due to temperature difference.

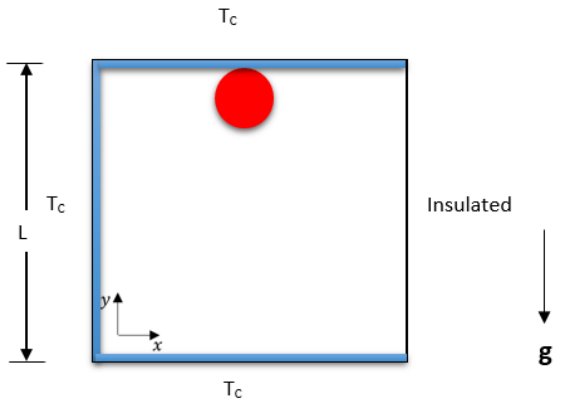


**Fig. 1** Schematic diagram of the configuration

Boussinesq approximation was utilized because of the assumption and with the thermal radiation neglected, a steady state natural convection has the governing equations of mass conservation, momentum and energy written thus:

$$\frac{\partial u}{\partial x}+\frac{\partial v}{\partial y}=0 \quad (1)$$

$$u\frac{\partial u}{\partial x}+v\frac{\partial u}{\partial y}=-\frac{1}{\rho}\frac{\partial P}{\partial x}+\vartheta\left\{\frac{\partial^2 u}{\partial x^2}+\frac{\partial^2 u}{\partial y^2}\right\} \quad (2)$$

$$u\frac{\partial v}{\partial x}+v\frac{\partial v}{\partial y}=-\frac{1}{\rho}\frac{\partial P}{\partial y}+\vartheta\left\{\frac{\partial^2 v}{\partial x^2}+\frac{\partial^2 v}{\partial y^2}\right\}+\beta g(T_h-T_c) \quad (3)$$

$$u\frac{\partial T}{\partial x}+v\frac{\partial T}{\partial y}=\propto\left(\frac{\partial^2 T}{\partial x^2}+\frac{\partial^2 T}{\partial y^2}\right) \quad (4)$$

Using the following dimensionless variables

$$P=\frac{pL^2}{\rho\propto} \quad X=\frac{x}{L} \quad R=\frac{r}{L} \quad Y=\frac{y}{L} \quad U=\frac{u\delta}{\propto}$$

$$V=\frac{v\delta}{\propto} \quad \theta=\frac{T-T_c}{T_h-T_c} \quad Pr=\frac{\vartheta}{\propto} \quad \Psi=\frac{\psi}{\propto}$$

$$Ra=\frac{\beta g(T_h-T_c)\delta^3 Pr}{\vartheta^2}$$

The resulting dimensionless form becomes

$$\frac{\partial U}{\partial X}+\frac{\partial V}{\partial Y}=0 \quad (5)$$

$$U\frac{\partial U}{\partial X}+V\frac{\partial U}{\partial Y}=-\frac{\partial P}{\partial X}+Pr\left\{\frac{\partial^2 U}{\partial X^2}+\frac{\partial^2 U}{\partial Y^2}\right\} \quad (6)$$

$$U\frac{\partial V}{\partial X}+V\frac{\partial V}{\partial Y}=-\frac{\partial P}{\partial Y}+Pr\left\{\frac{\partial^2 V}{\partial X^2}+\frac{\partial^2 V}{\partial Y^2}\right\}+RaPr\theta \quad (7)$$

$$U\frac{\partial \theta}{\partial X}+V\frac{\partial \theta}{\partial Y}=\propto\left(\frac{\partial^2 \theta}{\partial X^2}+\frac{\partial^2 \theta}{\partial Y^2}\right) \quad (8)$$

The governing convection parameters in equations above are Ra and Pr

For the dimensionless boundary conditions; P=0, U=V=0 at all boundaries

$\theta=1$ at cooled walls

$\frac{\partial \theta}{\partial Y}=0$ at the circular heated block

The motion of fluid is related by the stream function and velocity components resulting in the equation below

$$\left(\frac{\partial^2 \Psi}{\partial X^2}+\frac{\partial^2 \Psi}{\partial Y^2}\right)=\left(\frac{\partial U}{\partial X}+\frac{\partial V}{\partial Y}\right) \quad (9)$$

The heat transfer coefficient in terms of average Nusselt number on the heated circular block becomes

$$Nu=\frac{1}{\pi}\left(\int_0^{\frac{L}{2R}}-\frac{\partial T}{\partial X_{X=0}}dY+\int_0^{\frac{L}{2R}}\frac{\partial T}{\partial X_{X=L/2R}}dY\right) \quad (10)$$

## 3. NUMERICAL SOLUTION

A CFD software package of COMSOL Multiphysics was employed to solve numerically the governing partial differential equations alongside the boundary conditions. COMSOL Multiphysics is a solver of finite element (Dechaumphai (1999)) problems for simulation of several physics and engineering applications. The model user was set to incompressible Navier-Stokes application mode, Diffusion application mode and convection-conduction mode to solve the dimensionless equations of momentum and energy. In order to ensure stability, Galerkin least-squared method and P2-P1 Lagrange elements were employed. The solutions of the discretization were derived from the damped Newton Raphson method and parallel direct solver; the target set is $10^{-6}$ as the convergence criterion. The tested computational code presented an excellent result after considering a finer mesh size to maintain an accurate post processing.

### 3.1. Grid Independent Test

The effect of grid size on the results were investigated through grid refinement. See Fig. 2 for the model mesh. Different grid sizes were tested and the changes in the parameter of interest (Nusselt Number) were observed. When the Nusselt number remained approximately constant after successive changing of the grid size, then the grid size is acceptable and thus influence of grid size has been eliminated in the result. The grid sizes were varied from 0.005 to 0.00125 at a Ra=$2.8\times10^6$

Global Digital Central
ISSN: 2151-8629

as shown in the Table 1. The percentage relative changes in Nu with respect to the referenced Nu (Nu at mesh 4) are shown in the table. The absolute percentage relative changes in Nu are 17.49641, 5.824, and 1.6099. Further increase grid size does not change the Nu but oscillate within the actual value. Therefore, mesh 3 is accepted so as to reduce the computation time.

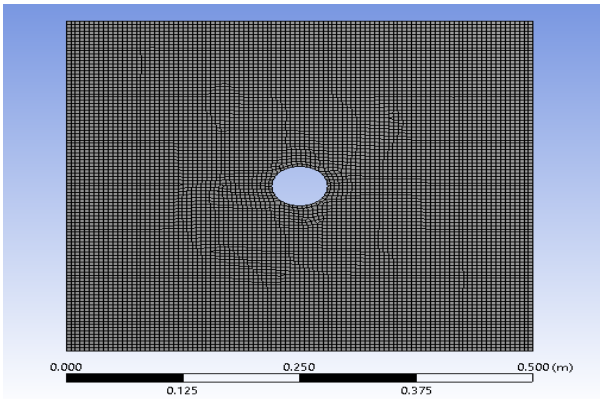


**Fig. 2** Model mesh

**Table 1** Grid independent testing

| *Mesh No.* | *Element size* | *Nu* |
|---|---|---|
| **1** | 0.005 | 145.1439 |
| **2** | 0.00375 | 130.725 |
| **3** | 0.0025 | 121.5417 |
| **4** | 0.00125 | 123.5305 |

### 3.2. Model Validation

It should be noted that due to lack of similar work in the literature and in order to validate the work, the present code was first developed for square cavity with embedded rectangular shape heated block and the solution was corroborated with the solution benchmark of Mousa (2010) for a square cavity heated at the vertical left wall and cooled at the opposite wall while the horizontal walls are kept insulated. The results of average Nusselt number of the present study shows an excellent agreement with the solutions of Mousa (2010) as shown in Table 2.

**Table1** The comparison of the average Nusselt number for code validations.

| **Ra** | **Present study** | **[4]** |
|---|---|---|
| $\mathbf{10^4}$ | 2.242 | 2.245 |
| $\mathbf{10^5}$ | 4.516 | 4.521 |
| $\mathbf{10^6}$ | 8.725 | 8.819 |

## 4. RESULTS AND DISCUSSION

### 4.1 Streamline formation and temperature contour

Numerical solution for convective heat transfer in a square cavity with embedded circular heated block at top, middle and bottom positions are described in form of streamline and temperature contours. The horizontal and left vertical walls maintained at cold temperature while the right vertical wall is insulated. Circular heated block within the cavity is kept at constant hot temperature. Rayleigh number were varied from $10^3$, $10^4$, $10^5$ and $10^6$ while the cavity room air temperature is fixed at Pr=0.7. Fig. 3 shows the streamline formation and temperature contours of circular block at the top of the cavity for Ra = $10^3$, $10^4$, $10^5$ and $10^6$.

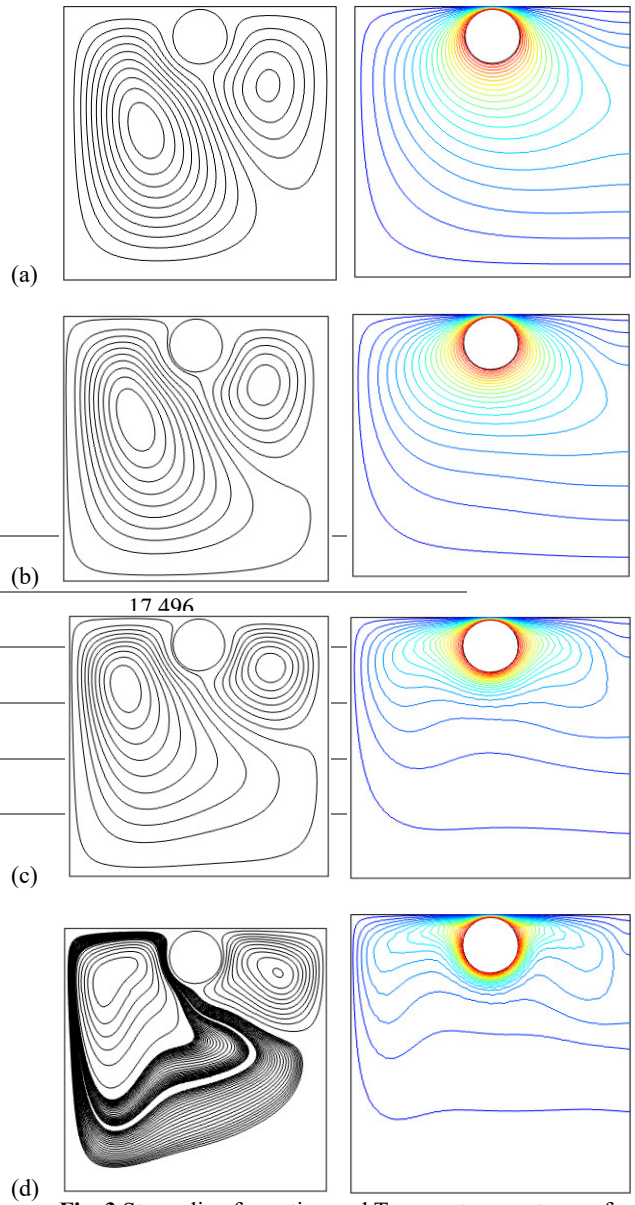


**Fig. 3** Streamline formation and Temperature contours of circular block at the top for (a). Ra=$10^3$ (b) Ra=$10^4$ (c) Ra=$10^5$ (d) Ra=$10^6$

The streamline formation at the left side represented in Fig. 3 shows the effect of increasing Rayleigh number on fluid flow and temperature distribution, two vortices around the hot circular body form a conduction dominated cavity, the larger vortex is due to the surrounding cold temperature at the top and left wall. Interestingly, at Ra=$10^3$ the fluid in the cavity is almost dominated by conduction heat transfer. As the Ra increases, the streamline at the larger vortex further thickens while the opposite vortex increases and further shrinks due to the increase in velocity of the fluid within the cavity. This scenario is vividly a demonstration of convective heat transfer characteristics.

The temperature contours at the right side of Fig. 3 reveals isothermal lines formed around the heated circular block and later

Global Digital Central
ISSN: 2151-8629

directed towards the insulated part of the cavity. The almost parallel isothermal lines show a low buoyancy driven force within the cavity of the embedded block. However, with Ra increasing, the contour reduces and becomes distorted due to the increase in driven buoyancy experienced around the embedded hot cavity which demonstrate a convection mode of heat transfer.

Fig. 4 reveals the stream line formation of the embedded body as positioned at the middle of cavity, the circular body is surrounded by recirculation of eddied at a lower Ra number symbolizing a conduction mode. The vortex is observed to split into two as the Ra increases and further thickens along the insulated walls, heat transferred from the embedded body at the middle has significantly affected the buoyancy driven force in the cavity converting the cavity from conduction mode to convection mode as the Ra increases.

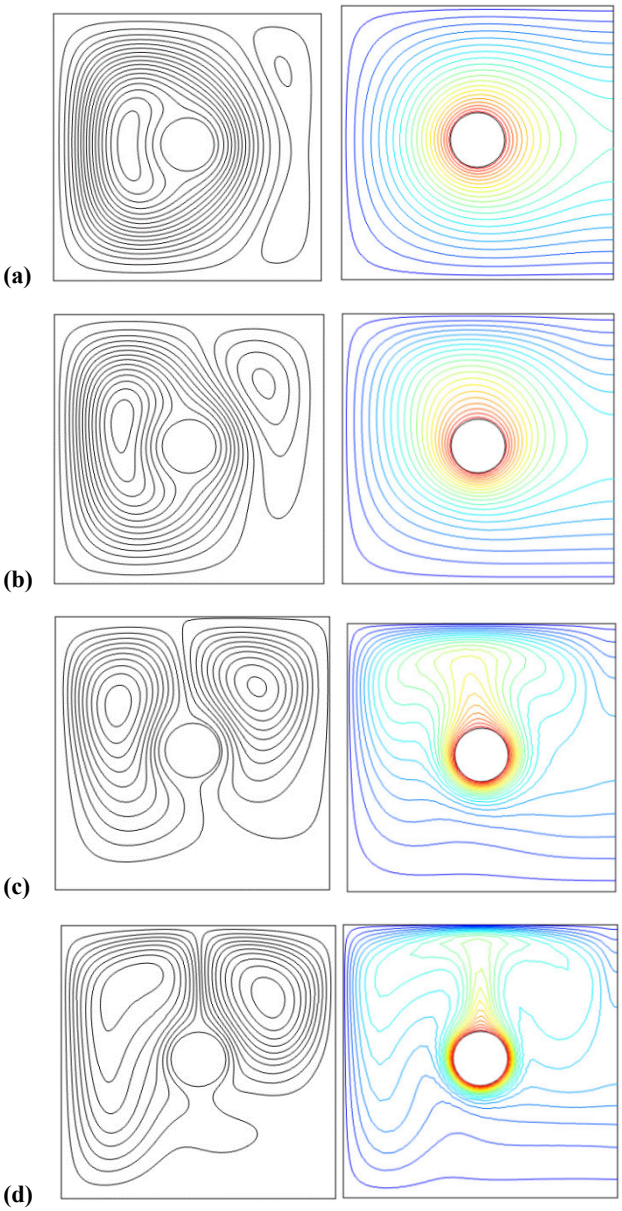


**Fig. 4** Stream line formation and Temperature contours of circular block at the middle for (a). Ra=$10^3$ (b) Ra=$10^4$ (c) Ra=$10^5$ (d) Ra=$10^6$

Further observed in Fig. 4 is that the temperature contours become parallel to the cold walls of the cavity due to high density of air in the cavity as a result of conduction heat transfer. The increase Ra causes the contours to distort vertically and spread to either sides of the walls because the buoyancy driven force has greatly influenced the heat transfer rate in the cavity turning the cavity to a convection mode at high Ra number.

The streamline formation and temperature contours of the phenomenon when the hot circular block is at the bottom of the cavity are depicted in Fig. 5. The streamline in the Fig. show that two vortices are formed at the opposite sides of the embedded circular block, one vortex being larger than the other. The larger vortex is as a result of the cold temperature applied at the left horizontal walls of the cavity causing a minimized velocity of fluid flow which makes the cavity to be conduction dominated at Ra=$10^3$. However, the smaller vortex gradually reduces as the Ra number increases to $10^6$ within the cavity, hence the influence of the buoyancy force is felt as the Ra number increases.

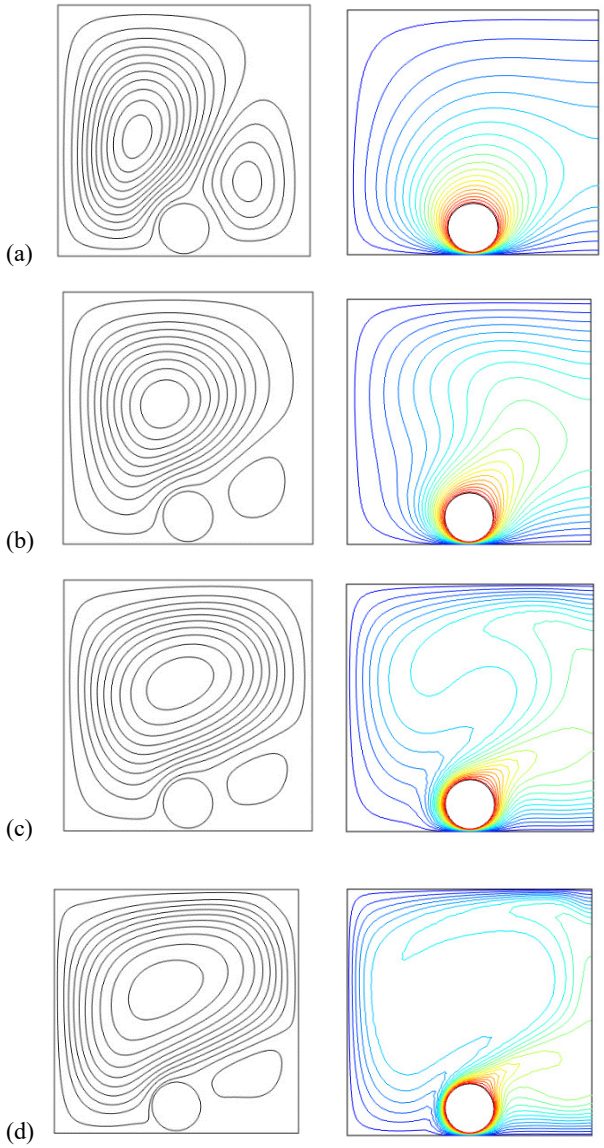


**Fig. 5** Stream line formation and Temperature contours of circular block at the bottom for a). Ra=$10^3$ b) Ra=$10^4$ c) Ra=$10^5$ d) Ra=$10^6$

The effect of the embedded body in the cavity positioned at the bottom is demonstrated by the temperature contour in Fig. 5(right). It should be noted that at Ra=$10^3$ isotherms are vertical along the cold left wall and observed to be horizontally parallel to the cold top wall and directed towards the insulated surface at the right wall of the cavity. Interestingly, as the Ra number increases, isotherms begin to distort as the velocity of the fluid gains energy as a result of the high buoyancy

force. The heat generated by the embedded block causes heat transfer by convection to be experienced in the cavity at Ra=$10^6$.

### 4.2 Distribution of Nusselt Number

The previous streamline formation and temperature contours showed that the heat transfer characteristics of the cavity depend strongly on the position of the embedded circular heated block. In order to further understand the phenomenon, the distribution of the Nusselt number along the horizontal wall for various Ra and at a specific position of the embedded body in the cavity is shown in Fig. 6, 7 and 8 for top, middle and bottom position, respectively. Interestingly negative Nusselt number is very pronounced at all Ra and for all positions. This might suggest a drift in the temperature gradient as a result of direction of heat flux. Fig. 6 suggest that the Nusselt number reduces as the Rayleigh number increases at either sides of the embedded circular block. However, only at Ra=$10^6$ is observed within the boundary of the embedded hot body. This reveals high velocity of fluid flows around the hot body at higher Ra number. Fig. 7 and 8 demonstrates a change in heat transfer as the Ra increases and subsequent reduction is observed in heat transfer coefficient along the horizontal walls of the cavity.

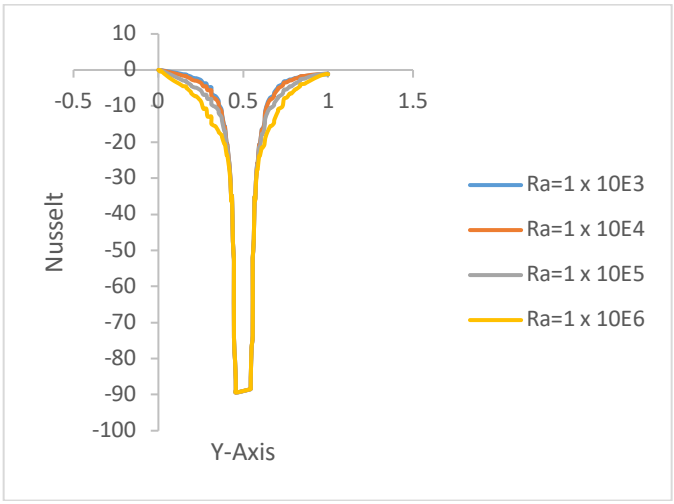


**Fig. 6** Distribution of Nusselt number along the horizontal wall at 0.99 top circular block position for various Ra

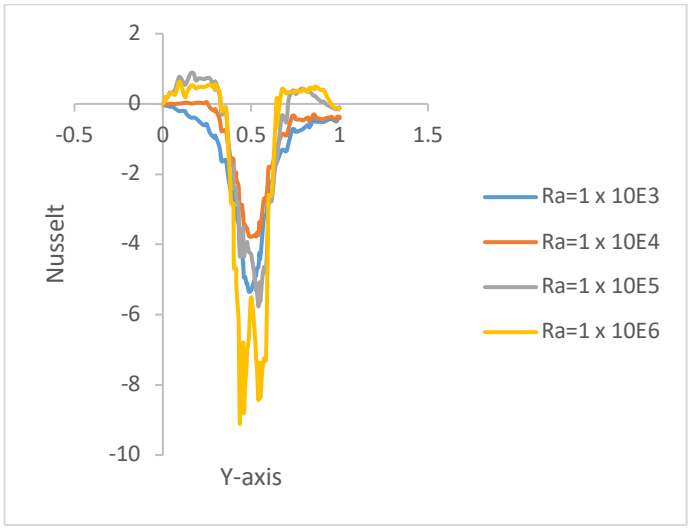


**Fig. 7** Distribution of Nusselt number along the horizontal wall at 0.62 middle circular block position for various Ra

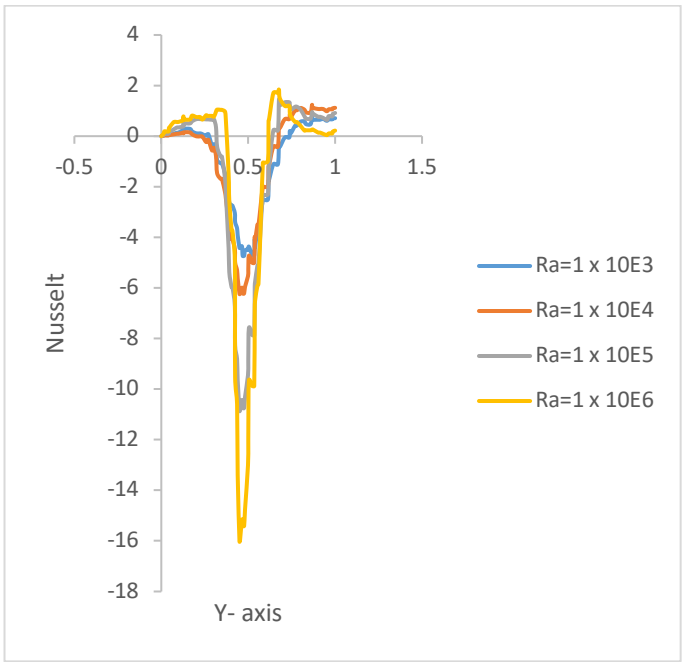


**Fig. 8** Distribution of Nusselt number along the horizontal wall at 0.22 bottom circular block position for various Ra

The evolution of the Nusselt number with the positions of the circular heated block at a fixed Ra is shown in Fig. 9, 10, 11 and 12 for Ra = $10^3$, $10^4$, $10^5$ and $10^6$ respectively. It should be noted that the wavelength and oscillation of the distributions follows similar pattern for all the Ra considered. Nevertheless, at a fixed Ra number, the Fig. reveals a dramatic change in Nusselt number along the horizontal walls of the cavity as the embedded body positioned changes which represent convection mode of heat transfer as a result of high fluid velocity.

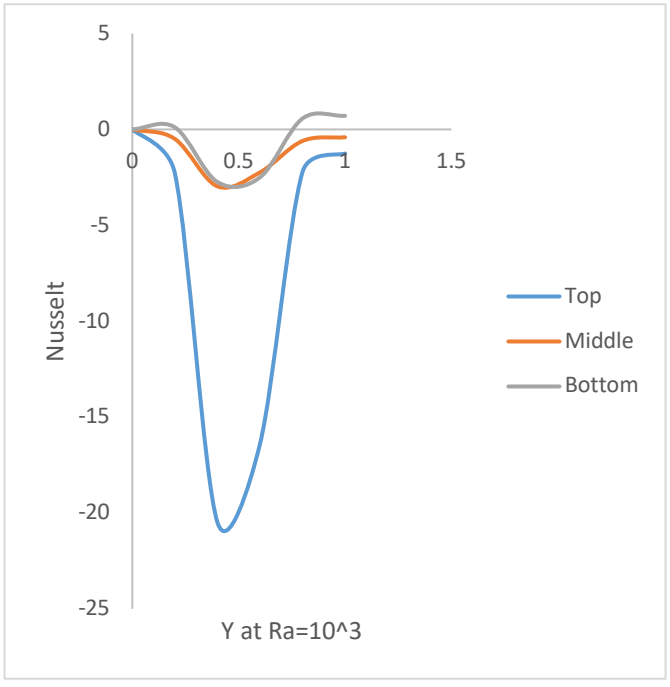


**Fig. 9** Variation of Nusselt number at Ra =$10^3$ for top, middle and bottom circular block position

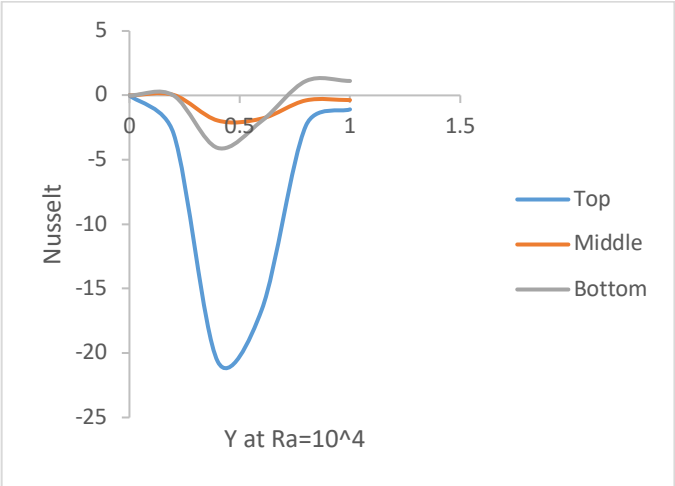


**Fig. 10** Variation of Nusselt number at Ra =$10^4$ for top, middle and \ bottom circular block position

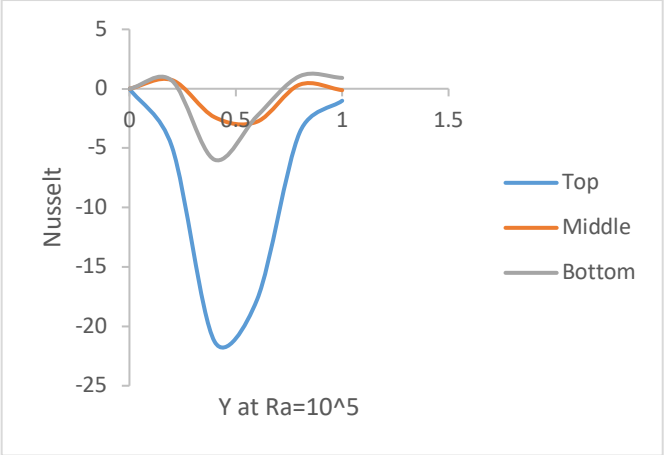


**Fig. 11** Variation of Nusselt number at Ra =$10^5$ for top, middle and bottom circular block position

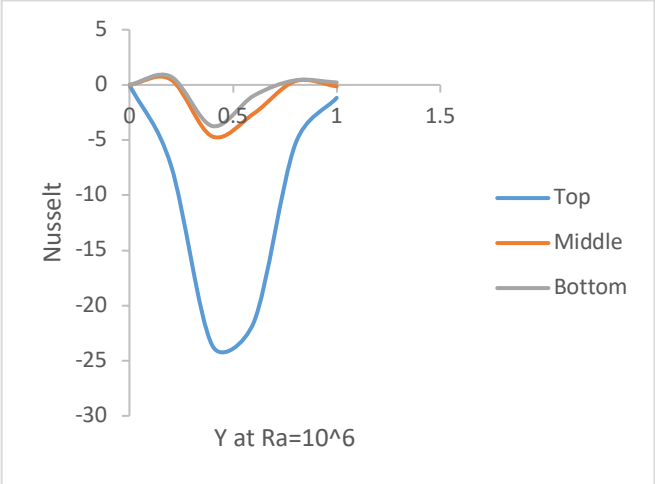


**Fig. 12** Variation of Nusselt number at Ra =$10^6$ for top, middle and bottom circular block position

## 5. CONCLUSIONS

A numerical analysis has been conducted for a steady state, laminar, incompressible convective heat transfer in a square cavity containing embedded circular heated block at different positions through the use of COSMOL Multiphysics software which employed finite element method to solve equations of mass, momentum and energy. Results are obtained for stream lines formation and temperature contours for varying parameters of Rayleigh number at the different location of the embedded circular heated block. The summary of the major observations can be stated thus:

i) The orientation of the embedded circular body has a tangible effect on the thermal fields and fluid flow characteristics.

ii) Thermal fields and fluid flow dramatically influenced the Rayleigh number. The increase in Rayleigh number significantly increased the Nusselt number.

iii) The position of the circular block in the cavity significantly affected the heat transfer rate from conduction dominant to convection mode.

iv) At a fixed Rayleigh number, the absolute Nusselt number dramatically increases when the circular body was embedded at the top position of the cavity.

v) For a fixed embedded circular body at any position in the cavity, Rayleigh number increases with increased Nusselt number along the horizontal walls of the cavity

**Nomenclatures**

| | | |
|---|---|---|
| u | Velocity in x-direction | v |
| | velocity in y-direction | |
| Ra | Rayleigh number | Pr |
| | Prandtl number | |
| $\alpha$ | Thermal diffusivity | $\vartheta$ |
| | Dynamic viscosity | |
| $g$ | Acceleration due to gravity | $T_c$ |
| | Cold temperature | |
| $T_h$ | Hot temperature | β |
| | volumetric thermal expansion | |
| $\Psi$ | Stream function | L |
| | Height of the enclosure | |
| P | Pressure | ρ |
| | Density | |
| Nu | Nusselt number | φ |
| | Interpolation function | |
| $R^n$ | Residual function | |
| $\Omega$ | Vorticity | Y |
| Dimensionless y length | | X |
| Dimensionless x length | | θ |
| dimensionless temperature | | |

## REFERENCES

Amnart, B. and Withada J, 2022, "Heat Transfer and Flow Profiles in Round Tube Heat Exchanger Equipped with Various V-Rings",,*Frontiers in Heat and Mass Transfer*, **18**, 2. http://dx.doi.org/10.5098/hmt.18.2.

Chowdhury, R., Khan, M. A. H.and Siddiki, M. N. A. A., 2005, "Natural Convection in Porous Triangular Enclosure with a Circular Obstacle in Presence of Heat Generation", *American Journal of Applied Mathematics*, **3 (2)**, 51-58. https://doi.org/10.11648/j.ajam.20150302.14.

Global Digital Central
ISSN: 2151-8629

Dechaumphai, P., 1999, "Finite Element Method in Engineering", 2nd ed. *Chulalongkorn University Press, Bangkok*.

Elyazid, F., Mohammed, S., Driss, A., and Mohamed E.,, 2021, "CFD Analysis of Free Convection in Non-Darcian Porous Medium and Comparison with Similarity Approach", *Frontiers in Heat and Mass Transfer*, **17**, 7. http://dx.doi.org/10.5098/hmt.17.7.

Kakali, C., Abdul, A. and Murad, H., 2019, "Natural Convection in a Partially Heated and Cooled Square Enclosure Containing a Diamond Shaped Heated Block", *International Journal of Fluid Mechanics & Thermal Sciences*, **6**, 1-8. https://doi.org/10.11648/j.ijfmts.20200601.11.

Kandaswamy, P., Lee, J. and Hakeem A. K. A., 2007, "Natural convection in a square cavity in presence of heated plate", *Nonlinear Analysis, Modeling and Control*, **12**, 203-212. https://doi.org/10.15388/NA.2007.12.2.14711.

Ha, M.Y., Kim, I. K. and Yoon, H. S., 2002, "Two-dimensional and unsteady natural convection in a horizontal enclosure with a square body", *Numerical Heat Transfer A: Applications*, **41**, 183–210. https://doi.org/10.1080/104077802317221393.

House, J. M., Beckermann, C. and Smith, T. F., 1990, "Effect of a centered conducting body on natural convection heat transfer in an enclosure", *Numerical Heat Transfer A: Applications*, **18**, 213–225. https://doi.org/10.1080/10407789008944791.

Mahmud, H. A. and Rawand, E. J., 2020, "Natural Convection in a Square Enclosure with Different Openings and Involves Two Cylinders: A Numerical Approach", *Frontiers in Heat and Mass Transfer*, **15**, 27. http://dx.doi.org/10.5098/hmt.15.27.

Merrikh, A.A. and Mohamad, A.A., 2001, "Blockage effects in natural convection in differentially heated enclosures", *Journal of Enhanced Heat Transfer*, **8 (1)**, 55–72. https://doi.org/10.1615/JEnhHeatTransf.v8.i1.50.

Mousa, M. M., "Modeling of laminar buoyancy convection in a square cavity containing an obstacle", *Mathematics Subject Classification*: **65**. https://doi.org/10.1007/s40840-015-0188-z.

Oyewola, O.M., Afolabi, S.I. and Ismail, O.S., 2021, "Numerical Simulation of Natural Convection in Rectangular Cavities with Different Aspect Ratios", *Frontiers in Heat and Mass Transfer*, **17**, 11. http://dx.doi.org/10.5098/hmt.17.11.

Parvin, S. and Nasrin, R., 2011, "Analysis of the flow and heat transfer characteristics for MHD free convection in an enclosure with a heated obstacle", *Nonlinear Analysis: Modeling and Control*, **16**, 89-99. https://doi.org/10.15388/NA.16.1.14117.

Roslan, R., Saleh, I.H., Hashim, I., 2014, "Natural Convection in a Differentially Heated Square Enclosure with a Solid Polygon", *The Scientific World Journal*. http://dx.doi.org/10.1155/2014/617492.

Saddam, A. M., 2020, "Effects of Variable Viscosity on Heat and Mass Transfer by MHD Mixed Convection Flow along a Vertical Cylinder Embedded In a Non-Darcy Porous Medium", *Frontiers in Heat and Mass Transfer*, **14**, 7. http://dx.doi.org/10.5098/hmt.14.7.

Santhi, K. D., Venkata, S. S. and Kishore P. M., 2021," Numerical Solution of the Effects of Heat And Mass Transfer on Unsteady MHD Free Convection Flow Past an Infinite Vertical Plate", *Frontiers in Heat and Mass Transfer*, **16**, 24. http://dx.doi.org/10.5098/hmt.16.24.

Shih, Y. C., Khodadadi, J. M., Weng, K. H. and Ahmed, A., 2009, "Periodic fluid flow and heat transfer in a square cavity due to an insulated or isothermal rotating cylinder", *Journal of Heat Transfer*, **131**, 1–11. https://doi.org/10.1115/1.3154620.

Zainab, K. G. and Ahmed, K. H., 2022, "Natural Convection in a Partially Heated Parallelogrammical Cavity with V-Shaped Baffle and Filled With Various Nanofluids", *Frontiers in Heat and Mass Transfer*, **18**, 6. http://dx.doi.org/10.5098/hmt.18.6.